DRAMA: MAMBA-ENABLED MODEL-BASED REINFORCEMENT LEARNING IS SAMPLE AND PARAMETER EFFICIENT

Anonymous authors
Paper under double-blind review

ABSTRACT

Model-based reinforcement learning (RL) offers a solution to the data inefficiency that plagues most model-free RL algorithms. However, learning a robust world model often demands complex and deep architectures, which are expensive to compute and train. Within the world model, dynamics models are particularly crucial for accurate predictions, and various dynamics-model architectures have been explored, each with its own set of challenges. Currently, recurrent neural network (RNN) based world models face issues such as vanishing gradients and difficulty in capturing long-term dependencies effectively. In contrast, use of transformers suffers from the well-known issues of self-attention mechanisms, where both memory and computational complexity scale as $O(n^2)$, with n representing the sequence length.

To address these challenges we propose a state space model (SSM) based world model, specifically based on Mamba, that achieves $O(n)$ memory and computational complexity while effectively capturing long-term dependencies and facilitating the use of longer training sequences efficiently. We also introduce a novel sampling method to mitigate the suboptimality caused by an incorrect world model in the early stages of training, combining it with the aforementioned technique to achieve a normalised score comparable to other state-of-the-art model-based RL algorithms using only a 7 million trainable parameter world model. This model is accessible and can be trained on an off-the-shelf laptop.

1 INTRODUCTION

Deep Reinforcement Learning (RL) has achieved remarkable success in various challenging applications, such as Go (Silver et al., 2016; 2017), Dota (Berner et al., 2019), Atari (Mnih et al., 2013; Schrittwieser et al., 2020), and MuJoCo (Schulman et al., 2017; Haarnoja et al., 2018). However, training policies capable of solving complex tasks often requires millions of interactions, which can be impractical and poses a barrier to real-world applications. Thus, improving sample efficiency has become one of the most critical goals in RL algorithm development.

World models have shown promise in improving sample efficiency through an autoregressive process that produces artificial samples on which to train RL agents, a method referred to as model-based RL (Micheli et al., 2023; Robine et al., 2023; Zhang et al., 2023; Hafner et al., 2024). In this approach, interaction data is used to learn the environment dynamics using a sequence model, allowing the agent to train on artificial experiences generated by the resulting dynamics model instead of relying on real-world interactions. This approach shifts the problem from improving the policy directly using real samples (which is sample inefficient) to improving the accuracy of the world model to match the real environment (which is more sample efficient). However, model-based RL faces a well-known challenge: when the model is inaccurate due to limited observed samples, especially early in training, the learned policy can become biased towards suboptimal behaviour, and detecting model errors is difficult, if not impossible.

In sequence modelling, linear complexity is highly desirable because it allows models to efficiently process longer sequences without a dramatic increase in computational and memory resources. This is particularly important when training world models, which require efficient sequence modelling

to simulate complex environments over long time horizons. Recurrent Neural Networks (RNNs), particularly advanced variants like Long Short-Term Memory (LSTM) and Gated Recurrent Units (GRU), offer linear complexity, making them computationally attractive for this task. However, RNNs still struggle with vanishing gradient issues and are inefficient in capturing long-term dependencies (Hafner et al., 2019; 2024). More recently, transformer architectures, which have dominated natural language processing (Vaswani et al., 2017), quickly gained widespread popularity in fields such as image processing and offline RL following groundbreaking work in these areas (Dosovitskiy et al., 2021; Chen et al., 2021). The transformer structure has demonstrated its effectiveness in model-based RL as well (Micheli et al., 2023; Robine et al., 2023; Zhang et al., 2023). However, transformers suffer from both memory and computation complexity that scale as $O(n^2)$, where n is the sequence length, creating challenges for world models that require long sequences to simulate complex environments.

Currently, State Space Models (SSMs) are attracting significant attention for their ability to efficiently handle long-sequence problems with linear complexity. Among SSMs, Mamba has emerged as a strong competitor to transformer-based architectures in various fields, including natural language processing (Gu & Dao, 2024; Dao & Gu, 2024), computer vision (Zhu et al., 2024), and offline RL (Ota, 2024). Applying Mamba's architecture to model-based RL is particularly appealing due to its linear memory and computational scaling with sequence length, while also effectively capturing long-term dependencies. Moreover, efficiently capturing environmental dynamics can reduce the likelihood that the behaviour policy is learned within an inaccurate world model, which we also address by incorporating a novel dynamic frequency-based sampling method. In this paper, we make three key contributions:

- We introduce Drama, the first model-based RL agent built on the Mamba SSM, with Mamba-2 as the core of its architecture. We evaluate Drama on the Atari100k benchmark, demonstrating that it achieves performance comparable to other state-of-the-art algorithms while using only a 7 million trainable parameter world model.
- Additionally, we compare the performance of Mamba-1 and Mamba-2, demonstrating that Mamba-2 achieves superior results as a dynamics model in the Atari100k benchmarks, despite it slightly limiting expressive power in order to enhance training efficiency.
- Finally, we propose a novel but straightforward sampling method, i.e., dynamic frequency-based sampling (DFS), to mitigate the challenges posed by imperfect dynamics models.

2 METHOD

We describe the problem as a Partially Observable Markov Decision Process (POMDP), where at each discrete time step t, the agent observes a high-dimensional image $\mathbf{O}_t \in \mathbb{O}$ rather than the true state $s_t \in \mathbb{S}$ with the conditional observation probability given by $p(\mathbf{O}_t|s_t)$. The agent selects actions from a discrete action set $a_t \in \mathbb{A} = \{0, 1, \ldots, n\}$. After executing an action a_t, the agent receives a scalar reward $r_t \in \mathbb{R}$, a termination flag $e_t \in [0, 1]$, and the next observation $\mathbf{O}_{t+1}$. The dynamics of the MDP is described by the transition probability $p(s_{t+1}, r_t|s_t, a_t)$. The behaviour of the agent is determined by a policy $\pi(\mathbf{O}_t; \boldsymbol{\theta})$, parameterised by $\boldsymbol{\theta}$, where $\pi : \mathbb{O} \to \mathbb{A}$ maps the observation space to the action space. The goal of this policy is to maximise the expected sum of discounted rewards $\mathbb{E} \sum_t \gamma^t r_t$, given that γ is a predefined discount factor.

Unlike model-free RL, model-based RL does not rely directly on real experiences to improve the policy $\pi(\mathbf{O}_t; \boldsymbol{\theta})$ (Sutton & Barto, 1998). There are various approaches to obtaining a world model, including Monte Carlo tree search Schrittwieser et al. (2020), offline imitation learning DeMoss et al. (2023) and latent dynamics models Hafner et al. (2019). In this work, we focus on learning a world model $f(\mathbf{O}_t, a_t; \omega)$ from actual experiences to capture the dynamics of the POMDP in a latent space. The actual experiences are stored in a replay buffer, allowing them to be repeatedly sampled for training the world model. The world model consists of a variational autoencoder (VAE) (Kingma & Welling, 2013; Hafner et al., 2021), a dynamics model, and linear heads to predict rewards and termination flags. The details of our world model are discussed in Section 2.2.

Each time the world model has been updated, a batch of experiences is sampled from the replay buffer to initiate a process called 'imagination'. Starting from an actual initial observation and using

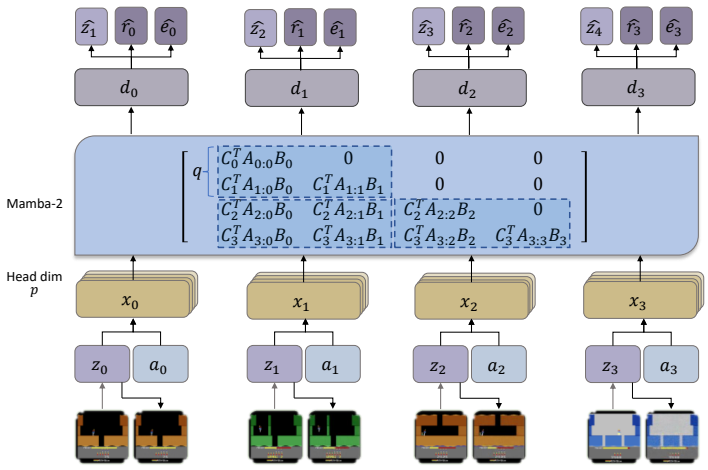

Figure 1: Drama world model architecture. Starting from sequence index t, the raw gaming frames are encoded into $\boldsymbol{z}_t$ and combined with the action a_t as input to the Mamba blocks. The input channel dimension is divided by the head dimension p to generate the deterministic recurrent state d_t. This recurrent state d_t is used to predict the next embedding $\hat{\boldsymbol{z}}_{t+1}$, reward $\hat{r}_t$, and termination flag $\hat{e}_t$, which represent the outcomes based on the current frame and action. The decoder reconstructs the original frame from the encoded embeddings $\boldsymbol{z}_t$ rather than from the predicted embeddings $\hat{\boldsymbol{z}}_t$. The Mamba-2 block employs a semiseparable matrix structure, which can be decomposed into $q \times q$ submatrices, enabling more efficient computation and processing.

an action generated by the current behaviour policy, the dynamics model generates the next latent state. This process is repeated until the agent collects enough imagined samples to improve the policy. We explain this process in detail in Section 2.3.

2.1 State Space Modelling with Mamba

SSMs are mathematical constructs inspired by control theory to represent the complete state of a system at a given point in time. These models map an input sequence to an output sequence $\boldsymbol{x} \in \mathbb{R}^l \rightarrow \boldsymbol{y} \in \mathbb{R}^l$, where l denotes the sequence length. In structured SSMs, a hidden state $\boldsymbol{H} \in \mathbb{R}^{(n,l)}$ is used to track the sequence dynamics, as described by the following equations:

$$\begin{aligned} \boldsymbol{H}_t &= \boldsymbol{A}\boldsymbol{H}_{t-1} + \boldsymbol{B}x_t \\ y_t &= \boldsymbol{C}^\intercal \boldsymbol{H}_t \end{aligned} \tag{1}$$

where $\boldsymbol{A} \in \mathbb{R}^{(n,n)}, \boldsymbol{B} \in \mathbb{R}^{(n,1)}, \boldsymbol{C} \in \mathbb{R}^{(n,1)}$ and $\boldsymbol{H}_t \in \mathbb{R}^{(n,1)}$, in which n represents the predefined dimension of the hidden state that remains invariant to the sequence length. To efficiently compute the hidden states, it is common to structure $\boldsymbol{A}$ as a diagonal matrix, as discussed in (Gu et al., 2022b; Gupta et al., 2022; Smith et al., 2023; Gu & Dao, 2024). Additionally, selective SSMs, such as Mamba-1, extend the matrices $(\boldsymbol{A}, \boldsymbol{B}, \boldsymbol{C})$ to be time-varying, introducing an extra dimension corresponding to the sequence length. The shapes of these time-varying matrices are $\mathbf{A} \in \mathbb{R}^{(T,N,N)}, \boldsymbol{B} \in \mathbb{R}^{(T,N)}$, and $\boldsymbol{C} \in \mathbb{R}^{(T,N)}$ [1].

Dao & Gu (2024) introduced the concept of structured state space duality (SSD), which further restricts the diagonal matrix $\boldsymbol{A}$ to be a scalar multiple of the identity matrix, forcing all diagonal elements to be identical. To compensate for the resulting reduced expressive power, Mamba-2 introduces a multi-head technique, akin to attention, by treating each input channel as p independent sequences. Unlike Mamba-1, which computes SSMs as a recurrence, Mamba-2 approaches the

[1] In Mamba-1, the time variation of $\boldsymbol{A}$ is influenced by a discretisation parameter Δ. For more details, please refer (Gu & Dao, 2024)

sequence transformation problem through matrix multiplication, which is more GPU-efficient:

$$\begin{aligned} y_t &= \boldsymbol{C}_t^\intercal \boldsymbol{H}_t \\ y_t &= \sum_{i=0}^{t} \boldsymbol{C}_t^\intercal \boldsymbol{A}_{t:i} \boldsymbol{B}_i x_i \end{aligned} \tag{2}$$

where $\boldsymbol{A}_{t:i}$ is $\boldsymbol{A}_t \boldsymbol{A}_{t-1} \dots \boldsymbol{A}_{i+1}$. This allows the SSM to be formulated as a matrix transformation:

$$\begin{aligned} \boldsymbol{y} &= SSM(\boldsymbol{x}; \mathbf{A}, \boldsymbol{B}, \boldsymbol{C}) = \boldsymbol{M} x \\ M_{j,i} &\coloneqq \begin{cases} \boldsymbol{C}_t^\intercal \boldsymbol{A}_{t:i} \boldsymbol{B}_i & \text{if } j \geq i \\ 0 & \text{if } j < i \end{cases} \end{aligned} \tag{3}$$

Mamba-2 reformulates the state-space equations as a single matrix multiplication by utilising semi-separable matrices (Vandebril et al., 2005; Dao & Gu, 2024), which is well known in computational linear algebra as shown by Figure 1. The matrix $\boldsymbol{M}$ can also be written as:

$$\begin{aligned} \boldsymbol{M} &= \boldsymbol{L} \circ \boldsymbol{C}\boldsymbol{B}^\intercal \in \mathbb{R}^{(T,T)} \\ \boldsymbol{L} &= \begin{bmatrix} 1 & & & & \\ a_1 & 1 & & & \\ a_2 a_1 & a_2 & 1 & & \\ \vdots & \vdots & \ddots & \ddots & \\ a_{\mathrm{T}-1} \dots a_1 & a_{\mathrm{T}-1} \dots a_2 & \dots & a_{\mathrm{T}-1} & 1 \end{bmatrix} \end{aligned} \tag{4}$$

where $a_t \in [0, 1]$ is an input-dependent scalar. The matrix $\boldsymbol{L}$ connects the SSM mechanism with the causal self-attention mechanism by removing the softmax function and applying a mask matrix $\boldsymbol{L}$ to the 'attention-like' matrix. It is, in fact, equivalent to causal linear attention when all $a_t = 1$. As a result, Mamba-2 achieves 2-8 times faster training speeds than Mamba-1, while maintaining linear scaling with sequence length.

2.2 World Model Learning

Our world model has two main components: an auto-encoder and a dynamics model. Additionally it includes two MLP heads for reward and termination predictions. The architecture of the world model is illustrated in Figure 1.

2.2.1 Discrete Variational Auto-encoder

The autoencoder extends the standard variational autoencoder (VAE) architecture (Kingma & Welling, 2013) by incorporating a fully-connected layer to discretise the latent embeddings, consistent with previous approaches (Hafner et al., 2021; Robine et al., 2023; Zhang et al., 2023). The raw observation is a three-dimensional image, $\mathbf{O}_t \in [0, 255]^{(h,w,c)}$, at time step t. The encoder compresses the observation into a vector of discrete numbers, denoted as $\boldsymbol{z}_t \sim p(\boldsymbol{z}_t | \mathbf{O}_t)$. The decoder reconstructs the raw image, $\hat{\mathbf{O}}_t$, from $\boldsymbol{z}_t$. Gradients are passed directly from the decoder to the encoder using the straight-through estimator, bypassing the sampling operation during backpropagation (Bengio et al., 2013).

2.2.2 Dynamics Model

The dynamics model simulates the environment in the latent variable space, $\boldsymbol{z}_t$, using a deterministic state variable, $\boldsymbol{d}_t$. Since we are employing SSMs like Mamba-1 and Mamba-2, this should not be confused with the hidden states typically used by SSMs to track dynamics. At each time step t, the next token in the sequence is determined by both the current latent variable, $\boldsymbol{z}_t$ and the current action a_t. To integrate these, we first concatenate them and project the result using a fully-connected layer before passing it to the dynamics model. Given a sequence length l, the deterministic state is derived from all previous latent variables and actions. The dynamics model can be expressed as:

$$\begin{aligned} &\text{Dynamics model:} && \boldsymbol{d}_t = f(\boldsymbol{z}_{t-l:t}, a_{t-l:t}; \omega) \\ &\text{Latent variable predictor:} && \hat{\boldsymbol{z}}_{t+1} \sim p(\hat{\boldsymbol{z}}_{t+1} | \boldsymbol{d}_t; \omega) \end{aligned} \tag{5}$$

We implement the dynamics model with Mamba-2 (Dao & Gu, 2024). Specifically, each time a batch of samples, denoted as $\mathbf{O} \in [0, 255]^{(b,l,h,w,c)}$, is drawn from the experience buffer $\mathcal{E}$, where b represents batch size, l the sequence length, and h, w, c the image height, width, and channel dimension respectively. After encoding, the batch will be compressed to $\mathbf{Z} \in \mathbb{R}^{(b,l,d)}$ where d is the dimension of the latent variable. The latent variable passes through a linear layer with the action to produce the input $\mathbf{X} \in \mathbb{R}^{(b,l,d)}$ of the Mamba blocks. To fully leverage the parallel computational capabilities of GPUs, the training process must not be strictly sequential. That is, at time step t, the dynamic model predicts the latent variable $\hat{\boldsymbol{z}}_{t+1}$, and its target $\boldsymbol{z}_{t+1}$ depends solely on the observation $\mathbf{O}_{t+1}$ as shown in Figure 1. Unlike DreamerV3, where $\boldsymbol{z}_{t+1} \sim p(\boldsymbol{z}_{t+1}|\mathbf{O}_{t+1}, \boldsymbol{d}_t)$, this approach does not have sequential dependence.

Mamba-1 first transforms the input tensor $\mathbf{X}_{b,:l,d}$ into a sequence of hidden states $\mathbf{H} \in \mathbb{R}^{(b,l-1,n)}$, which are then mapped back to the deterministic state sequence $\mathbf{D}_{b,:l,d}$ using time-varying parameters. Since the hidden states operate in a fixed dimension n (unlike standard attention mechanisms, where the state scales with the sequence length), Mamba-1 achieves linear computational complexity with respect to sequence length.

Mamba-2 applies a similar transformation but leverages matrix multiplication. The input tensor $\mathbf{X}$'s dimension d is first split into d/p heads, which are processed independently. The transformation matrix is a specially designed semiseparable lower triangular matrix, which can be decomposed into $q \times q$ blocks. Different types of blocks are designed for specific purposes, such as handling causal attention over short ranges and transforming the hidden states.

2.3 Behaviour Policy Learning

The behaviour policy is trained within the 'imagination', an autoregressive process driven by the dynamics model. Specifically, a batch of b_{img} trajectories each of length l_{img} is sampled from the replay buffer. Since the Mamba dynamics model is efficient at handling long sequences, we can leverage actual experiences to estimate a more informative hidden state for the 'imagination' process. The rollout begins from the last transition in each sequence, l_{img}, and continues for h steps. Notably, the rollout does not stop when an episode ends, unlike the prior SSM-based meta-RL model (Lu et al., 2023) where the hidden state must be manually reset, as the Mamba-based dynamics model automatically resets the state at episode boundaries (Gu & Dao, 2024).

A key difference between Mamba-based and transformer-based world models in the 'imagination' process is that Mamba updates inference parameters independently of sequence length. This independence is crucial for accelerating the 'imagination' process, a significantly time-consuming component in model-based RL. The behaviour policy's state concatenates the prior discrete variable $\hat{\boldsymbol{z}}_t$ with the deterministic variable $\boldsymbol{d}_t$ to exploit the temporal information. While the behaviour policy utilises a standard actor-critic architecture, other on-policy algorithms can also be applied. In this work, we adopt the recommendations from (Andrychowicz et al., 2020) and adjust the loss functions and value normalisation techniques as described in (Hafner et al., 2024).

2.4 Dynamic Frequency-Based Sampling (DFS)

In model-based RL, the behaviour model often underestimates rewards due to inaccuracies in the world model, impeding exploration and error correction (Sutton & Barto, 1998). These inaccuracies are particularly common early in training when the model relies on limited data. Thus, we propose a sample-efficient method to address this issue, i.e., Dynamic Frequency-based Sampling (DFS).

The primary objective is to sample transitions that the world model has sufficiently learned to initiate 'imagination'. To accomplish this, we introduce two vectors during training, each matching the length of the transition buffer $|\mathcal{E}|$. For the world model, $\boldsymbol{v} = (v_1, v_2, \ldots, v_{|\mathcal{E}|})$, where $v_i \in \mathbb{Z}^+$ for $i \in \{1, 2, \ldots, |\mathcal{E}|\}$, tracks how many times the transition has been used to improve the world model. The consequencing sampling probability is denoted as, $(p_1, p_2, \ldots, p_{|\mathcal{E}|}) = \texttt{softmax}(-\boldsymbol{v})$, this is similar to (Robine et al., 2023). For 'imagination', $\boldsymbol{b} = (b_1, b_2, \ldots, b_{|\mathcal{E}|})$, where $b_i \in \mathbb{Z}^+$ for $i \in \{1, 2, \ldots, |\mathcal{E}|\}$, counts the times that the transition has been used to improve the behaviour policy. The resulting sampling probability is denoted as, $(p_1, p_2, \ldots, p_{|\mathcal{E}|}) = \texttt{softmax}(f(\boldsymbol{v}, \boldsymbol{b}))$, where $f(\boldsymbol{v}, \boldsymbol{b}) = \boldsymbol{v} - \boldsymbol{b} - \max(0, \boldsymbol{v} - \boldsymbol{b})$. During training, two cases arise:

1) $\exists i \in |\mathcal{E}|, v_i \geq b_i, f(v_i, b_i) = 0$, In this case, the transition has been trained more frequently with the world model than with the behaviour policy, suggesting that the world model is likely capable of making accurate predictions from this transition. 2) $\exists i \in |\mathcal{E}|, v_i < b_i, f(v_i, b_i) = v_i - b_i$, indicating that the transition is either likely under-trained as a starting point for the world model generation process or has been over-fitted to the behaviour policy. Consequently, the probability of selecting this transition for behaviour policy training decreases. These two mechanisms ensure that 'imagination' sampling favors transitions learned by the world model, while avoiding excessive determinism.

3 EXPERIMENTS

In this work, the proposed Drama framework is implemented on top of the STORM infrastructure (Zhang et al., 2023). We evaluate the model using the **Atari100k benchmark** (Kaiser et al., 2020), which is widely used for assessing the sample efficiency of RL algorithms. Atari100k limits interactions with the environment to 100,000 steps (equivalent to 400,000 frames with 4-frame skipping). We present the benchmark and analyse our results in Section 3.1 . Ablation experiments and their analysis are provided in Section 3.2.

3.1 ATARI100K RESULTS

	Random	Human	PPO	SimPLe	SPR	TWM	IRIS	STROM	DreamerV3	DramaXS
Alien	228	7128	276	617	842	675	420	984	**1118**	820
Amidar	6	1720	26	74	180	122	143	**205**	97	131
Assault	222	742	327	527	566	683	**1524**	801	683	539
Asterix	210	8503	292	1128	962	1117	854	1028	1062	**1632**
BankHeist	14	753	14	34	345	467	53	**641**	398	137
BattleZone	2360	37188	2233	4031	14834	5068	13074	13540	**20300**	10860
Boxing	0	12	3	8	36	78	70	80	**82**	78
Breakout	2	30	3	16	20	20	**84**	16	10	7
ChopperCommand	811	7388	1005	979	946	1697	1565	1888	**2222**	1642
CrazyClimber	10780	35829	14675	62584	36700	71820	59324	66776	**83931**	52242
DemonAttack	152	1971	160	208	518	350	**2034**	165	577	201
Freeway	0	30	2	17	19	24	31	**34**	0	15
Frostbite	65	4335	127	237	1171	1476	259	1316	**3377**	785
Gopher	258	2412	368	597	661	1675	2236	**8240**	2160	2757
Hero	1027	30826	2596	2657	5859	7254	7037	11044	**13354**	7946
Jamesbond	29	303	41	100	366	362	463	509	**540**	372
Kangaroo	52	3035	55	51	3617	1240	838	**4208**	2643	1384
Krull	1598	2666	3222	2205	3682	6349	6616	8413	8171	**9693**
KungFuMaster	258	22736	2090	14862	14783	24555	21760	**26183**	23920	17236
MsPacman	307	6952	366	1480	1318	1588	999	**2673**	1521	2270
Pong	-21	15	-20	13	-5	**19**	15	11	-4	15
PrivateEye	25	69571	100	35	86	87	100	**7781**	3238	90
Qbert	164	13455	317	1289	866	3331	746	**4522**	2921	796
RoadRunner	12	7845	602	5641	12213	9109	9615	17564	**19230**	14020
Seaquest	68	42055	305	683	558	774	661	525	**962**	497
UpNDown	533	11693	1502	3350	10859	15982	3546	7985	**46910**	7387
Normalised Mean (%)	0	100	11	33	62	96	105	127	125	105
Normalised Median (%)	0	100	3	13	40	51	29	58	49	27

Table 1: Comparison of game performance metrics for various algorithms across multiple Atari games. For `Freeway` IRIS enhances exploration using a distinct set of hyperparameters, while STORM leverages offline expert knowledge. TWM reports the results with a 21.6M model while IRIS does not report the exact number of parameters, they use the same transformer embedding dimension and layer number as TWM plus a behaviour policy with CNN layers. DreamerV3 notably uses a 200M parameter model and achieves good results in a series of diverse tasks. STORM does not report the number of trainable parameters.

We compare our model against several benchmarks across 26 Atari games. In Table 1, the 'Normalised Mean' refers to the average normalised score, calculated as: $(evaluated\_score -$

$random\_score)/(human\_score - random\_score)$. For each game, we train Drama with 5 different seeds and track training performance using a running average of 5 episodes, as recommended by Machado et al. (2018), a practice also followed in related work (Hafner et al., 2024).

Despite utilising an extra-small world model (7M parameters, referred to as the XS model), Drama achieves performance comparable to IRIS and TWM. To enable a like-for-like comparison between Drama and DreamerV3 with a similar number of parameters, we evaluate the learning curves of Drama and a version of Dreamer with only 12M parameters (referred to as DreamerV3XS) on the full Atari100K benchmark. As shown in Figure 4 in the appendix, Drama demonstrates significantly better performance than DreamerXS, achieving a normalized mean score of 105 compared to 37 and a normalized median score of 27 compared to 7, as presented in Table 3.

Table 1 demonstrates that Drama, with Mamba-2 as the dynamics model, is both sample- and parameter-efficient. For comparison, Simple (Kaiser et al., 2020) trains a video prediction model to optimise a PPO agent (Schulman et al., 2017), while SPR (Schwarzer et al., 2021) uses a dynamics model to predict in latent space, enhancing consistency through data augmentation. TWM (Robine et al., 2023) employs a Transformer-XL architecture to capture dependencies among states, actions, and rewards, training a policy-based agent. This method incorporates short-term temporal information into the embeddings to avoid using the dynamics model during actual interactions. Similarly, IRIS (Micheli et al., 2023) uses a Transformer as its dynamics model, but generates new samples in image space, allowing pixel-level feature extraction for behaviour policies. DreamerV3 (Hafner et al., 2024), which employs an RNN-based dynamics model along with robustness techniques, achieves superhuman performance on the Atari100k benchmark using a 200M parameter model—20 times larger than our XS model. STORM (Zhang et al., 2023), which adopts many of DreamerV3's robustness techniques while replacing the dynamics model with a transformer, reaches similar performance on the Atari100k benchmark as DreamerV3.

Drama excels in games like `Boxing` and `Pong`, where the player competes against an autonomous agent in simple, static environments, requiring a less intense auto-encoder. This strong performance indicates that Mamba-2 effectively captures both ball dynamics and the opponent's position. Similarly, Drama performs well in `Asterix`, which benefits from its ability to predict object movements. However, Drama struggles in `Breakout`, where performance can be improved with a more robust auto-encoder in Figure 6. Additionally, Drama excels in games like `Krull` and `MsPacman`, which require longer sequence memory, but faces challenges in sparse reward games like `Jamesbond` and `PrivateEye`.

3.2 Ablation experiments

In this section, we present three ablation experiments to evaluate key components of Drama. First, we compare dynamic frequency-based sampling performance against uniform sampling on the full Atari100k benchmark, demonstrating its effectiveness across diverse environments. Secondly, we compare Mamba-1 and Mamba-2 on a subset of Atari games, including `Krull`, `Boxing`, `Freeway`, and `Kangaroo`, to highlight the differences in their performance when applied to dynamic gameplay scenarios. Lastly, we compare the long-sequence processing capabilities of Mamba-1, Mamba-2, and GRU in a custom Grid World environment. This experiment focuses on a prediction task using differnt dynamics models, offering insights into their sequence modelling capabilities, which are crucial for MBRL applications especially if long-sequence modelling is important.

3.2.1 Dynamic Frequency-Based Sampling

In this experiment, we compare DFS with the uniform sampling method in the Mamba-2-based Drama on the full Atari100k benchmark. As shown in Figure 5, DFS outperforms uniform sampling in 11 games, underperforms in 2 games, and performs equally in 13 games. These results demonstrate that applying DFS generally does not degrade performance and is often advantageous in the Atari100k task. DFS shows significant advantages in games like `Alien`, `Asterix`, `BankHeist`, and `Seaquest`, where adapting to game dynamics in the later stages is crucial. Additionally, DFS performs well in opponent-based games such as `Boxing` and `Pong`, where exploiting the weaknesses of the opponent AI is essential. However, DFS performs less effectively in games like

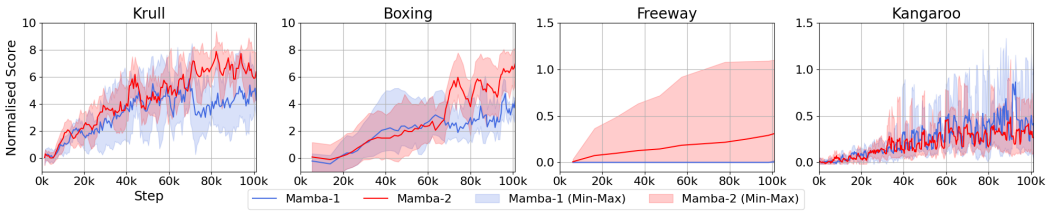

Figure 2: Mamba-1 vs. Mamba-2. Mamba2 has shown a superior performance over Mamba-1 three out of four games. Both Mamba-1 and Mamba-2 use DFS in this experiment.

`Breakout` and `KungFuMaster`, likely because the critical game dynamics are accessible early in the gameplay.

3.2.2 MAMBA-1 VS. MAMBA-2

As mentioned in Sec 2.1, Mamba-2 imposes restrictions on $\boldsymbol{A}$ for efficiency. However, it remains an open question whether these constraints negatively affect the performance of SSMs, as previous studies have not offered comprehensive theoretical or empirical evidence on the matter (Dao & Gu, 2024). In response to this gap, we compare Mamba-2 and Mamba-1 as the backbone of the world model in model-based RL. Ablation experiments were conducted using DFS, with both Mamba-1 and Mamba-2 configured with the same default hyperparameters.

Figure 2 illustrates that Mamba-2 outperforms Mamba-1 in games `Krull`, `Boxing` and `Freeway`. In `Krull`, the player navigates through different scenes and solves various tasks. In the later stages, rescuing the princess while avoiding hits results in a significant score boost, while failure leads to a plateau in score. As shown, Mamba-1 experiences a score plateau in `Krull`, whereas Mamba-2 successfully overcomes this challenge, leading to higher performance. Note that `Freeway` is a sparse reward game requiring high-quality exploration. A positive training effect is achieved only by combining DFS with Mamba-2 without any additional configuration.

3.2.3 DYNAMICS MODELS FOR LONG-SEQUENCE PREDICTABILITY TASKS

To assess the efficiency of Mamba-1 and Mamba-2 in long-range modelling compared to Transformers and GRUs, which are widely used in recent MBRL approaches, we present a simple yet representative grid world environment[2], as illustrated in Figure 3a. The learning objectives here are twofold: 1) the dynamics model must reconstruct (predict) the correct grid-world geometry over a long sequence and 2) the dynamics model must accurately generate the agent's location within the grid world, reflecting the prior sequence of movements. To achieve this, we represent a trajectory as a long sequence by flattening (successive) frames and separating each frame with a movement action a. Each frame is flattened row-wise, such that each cell is treated as a token. Let the size of the grid world be l_g. Then, each frame can be tokenized into a sequence of length $l_f = {l_g}^2 + 1$, as depicted in Figure 3b. Since $l \gg l_f$, the task demands that the dynamics model exhibit long-range sequence memory and modelling capabilities to accurately generate (predict) tokens that are both geometrically and logically consistent. The capability represents the core component of a MBRL dynamics model.

We evaluate the performance of GRU, Transformer, Mamba-1, and Mamba-2 based solutions in this grid world environment, where $l_g = 5$ and $l_f = 26$, considering two sequence lengths: a short sequence length $l = 8 \times l_f$ and a long sequence length $l = 64 \times l_f$. Performance is measured in terms of training time, memory usage and reconstruction error, where lower time consumption and reconstruction error indicate a stronger understanding of the environment. Experimental results show that, Mamba-1 and Mamba-2 achieve equivalent low error and short training time in both sequence lengths compared to other methods. However, Mamba-2 demonstrates the lowest training time over all methods. These findings confirm that the proposed Mamba-based architecture presents a strong capability to capture essential information, particularly in scenarios involving long sequence lengths.

[2]Implementation based on Torres–Leguet (2024)

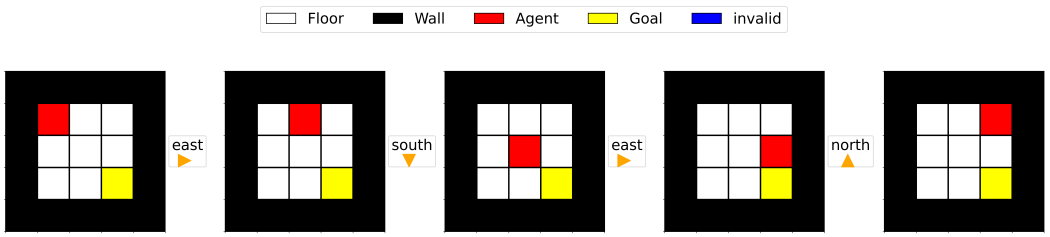

(a)

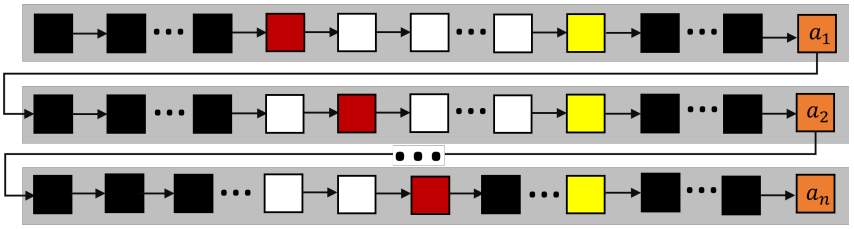

(b)

Figure 3: Illustrations of the grid world environment and its reconstruction into a sequential format. (a) Sequence of continuous frames in the grid world environment. Example presents a sequence of continuous frames, arranged from left to right. Each frame in the grid world environment represents a 5×5 grid, where the outer 16 cells are black walls, and the central 3×3 grid is the reachable space. The red cell is the controllable agent, which moves according to a random action, and the yellow cell is a fixed goal. The sequence of frames, from left to right, illustrates the movement of the agent following the action sequence: $east \rightarrow south \rightarrow east \rightarrow north$. Once the yellow cell is reached by the agent, the location of the agent and goal will be reset randomly. (b) Reconstructing the grid world into a long sequence. Each grey-shaded box contains 25 flattened grid tokens and one action token.

Method	l	**Training Time (ms)**	**Memory Usage (%)**	**Error (%)**
Mamba-2	208	25	13	15.6 ± 2.6
	1664	214	55	14.2 ± 0.3
Mamba-1	208	34	14	13.9 ± 0.4
	1664	299	52	14.0 ± 0.4
GRU	208	75	66	21.3 ± 0.3
	1664	628	68	34.7 ± 25.4
Transformer	208	45	17	75.0 ± 1.1
	1664	-	OOM	-

Table 2: Performance comparison of different methods on the grid world environment. Memory usage is reported as a percentage of an 8GB GPU. The error is represented as the mean $\pm$ standard deviation. The training time refers to the average duration of one training step. Note that the Transformer encounters an out-of-memory (OOM) error during training with long sequences. The experiments are conducted on a laptop. The definition of **Error (%)** can be found in Appendix A.6.

4 Related Work

4.1 Model-based RL

The origin of model-based RL can be traced back to the Dyna architecture introduced by Sutton & Barto (1998), although Dyna selects actions through planning rather than learning. Notably, Sutton & Barto (1998) also highlighted the suboptimality that arises when the world model is flawed, especially as the environment improves. The concept of learning in 'imagination' was first proposed by Ha & Schmidhuber (2018), where a world model predicts the dynamics of the environment. Later,

SimPLe (Kaiser et al., 2020) applied MBRL to Atari games, demonstrating improved sample efficiency compared to state-of-the-art model-free algorithms. Beginning with Hafner et al. (2019), the Dreamer series introduced a GRU-powered world model to solve a diverse range of tasks, such as Mujoco, Atari, Minecraft, and others (Hafner et al., 2020; 2021; 2024). More recently, inspired by the success of transformers in NLP, many MBRL studies have adopted transformer architectures for their dynamics models. For instance, IRIS (Micheli et al., 2023) encodes game frames as sets of tokens using VQ-VAE (Oord et al., 2018) and learns sequence dependencies with a transformer. In IRIS, the behavior policy operates on raw images, requiring an image reconstruction during the 'imagination' process and an additional CNN-LSTM structure to extract information. TWM (Robine et al., 2023), another transformer-based world model, uses a different structure. It stacks grayscale frames and does not activate the dynamics model during actual interaction phases. However, its behaviour policy only has access to short-term temporal information, raising questions about whether learning from tokens that already include this short-term information could be detrimental to the dynamics model. STORM (Zhang et al., 2023), closely following DreamerV3, replaces the GRU with a vanilla transformer. Additionally, it incorporates a demonstration technique, populating the buffer with expert knowledge, which has shown to be particularly beneficial in the game `Freeway`.

4.2 Structure State space model based RL

Structured SSMs were originally introduced to tackle long-range dependency challenges, complementing the transformer architecture (Gu et al., 2022a; Gupta et al., 2022). However, Mamba and its successor, Mamba-2, have emerged as powerful alternatives, now competing directly with transformers (Gu & Dao, 2024; Dao & Gu, 2024). Deng et al. (2023) implemented an SSM-based world model, comparing it against RNN-based and transformer-based models across various prediction tasks. Despite this, SSM-based world models have yet to be tested in the context of model-based RL, including Mamba-1 and Mamba-2. Mamba-1 has recently been applied to offline RL, either with a standard Mamba-1 block (Ota, 2024) or a Mamba-attention hybrid model (Huang et al., 2024). Lu et al. (2023) proposed applying modified SSMs to meta-RL, where hidden states are manually reset at episode boundaries. Since both Mamba-1 and Mamba-2 are input-dependent, such resets are unnecessary. Recall to Imagine (R2I) introduces advanced state space models to enhance long-term memory and credit assignment in MBRL, achieving state-of-the-art performance in challenging memory-intensive tasks while maintaining generality and faster convergence than DreamerV3 (Samsami et al., 2024).

5 Conclusion

In conclusion, Drama, our proposed Mamba-based world model, addresses key challenges faced by RNN and transformer-based world models in model-based RL. By achieving $O(n)$ memory and computational complexity, our approach enables the use of longer training sequences. Furthermore, our novel sampling method effectively mitigates suboptimality during the early stages of training, contributing to a model that is both lightweight, with only 7 million trainable parameter world model, and accessible, being trainable on standard hardware. Overall, our method achieves a normalised score competitive with other state-of-the-art RL algorithms, offering a practical and efficient alternative for model-based RL systems. Although Drama enables longer training and inference sequences, it does not demonstrate a decisive advantage that would allow it to dominate other world models on the Atari100k benchmark. An interesting direction for future work is to explore specific tasks where longer sequences drive superior performance in model-based RL. Despite advances in world models, model-based RL still faces several challenges, such as long-horizon behaviour planning and learning, informed exploration, and the dynamics of jointly training the world model and behaviour policy. Another promising future direction is to investigate to what extent Mamba can help address these challenges.

References

Marcin Andrychowicz, Anton Raichuk, Piotr Stańczyk, Manu Orsini, Sertan Girgin, Raphael Marinier, Léonard Hussenot, Matthieu Geist, Olivier Pietquin, Marcin Michalski, Sylvain Gelly, and Olivier Bachem. What Matters In On-Policy Reinforcement Learning? A Large-Scale Em-

pirical Study, June 2020. URL http://arxiv.org/abs/2006.05990. arXiv:2006.05990 [cs, stat].

Yoshua Bengio, Nicholas Léonard, and Aaron Courville. Estimating or Propagating Gradients Through Stochastic Neurons for Conditional Computation, August 2013. URL http://arxiv.org/abs/1308.3432. arXiv:1308.3432 [cs].

Christopher Berner, Greg Brockman, Brooke Chan, Vicki Cheung, Przemysław Dębiak, Christy Dennison, David Farhi, Quirin Fischer, Shariq Hashme, Chris Hesse, Rafal Józefowicz, Scott Gray, Catherine Olsson, Jakub Pachocki, Michael Petrov, Henrique P.d.O. Pinto, Jonathan Raiman, Tim Salimans, Jeremy Schlatter, Jonas Schneider, Szymon Sidor, Ilya Sutskever, Jie Tang, Filip Wolski, and Susan Zhang. Dota 2 with Large Scale Deep Reinforcement Learning, December 2019. URL http://arxiv.org/abs/1912.06680. arXiv:1912.06680 [cs, stat].

Lili Chen, Kevin Lu, Aravind Rajeswaran, Kimin Lee, Aditya Grover, Michael Laskin, Pieter Abbeel, Aravind Srinivas, and Igor Mordatch. Decision Transformer: Reinforcement Learning via Sequence Modeling. In *Advances in Neural Information Processing Systems 34*, pp. 15084–15097, June 2021.

Tri Dao and Albert Gu. Transformers are SSMs: Generalized Models and Efficient Algorithms Through Structured State Space Duality. In *Proceedings of the 41st International Conference on Machine Learning*, volume 235, pp. 10041–10071, 2024.

Branton DeMoss, Paul Duckworth, Nick Hawes, and Ingmar Posner. DITTO: Offline Imitation Learning with World Models, February 2023. URL http://arxiv.org/abs/2302.03086. arXiv:2302.03086.

Fei Deng, Junyeong Park, and Sungjin Ahn. Facing Off World Model Backbones: RNNs, Transformers, and S4. In *Advances in Neural Information Processing Systems*, volume 36, pp. 72904–72930, 2023.

Alexey Dosovitskiy, Lucas Beyer, Alexander Kolesnikov, Dirk Weissenborn, Xiaohua Zhai, Thomas Unterthiner, Mostafa Dehghani, Matthias Minderer, Georg Heigold, Sylvain Gelly, Jakob Uszkoreit, and Neil Houlsby. An Image is Worth 16x16 Words: Transformers for Image Recognition at Scale. In *International Conference on Learning Representations*, 2021.

Albert Gu and Tri Dao. Mamba: Linear-Time Sequence Modeling with Selective State Spaces, May 2024. URL http://arxiv.org/abs/2312.00752. arXiv:2312.00752 [cs].

Albert Gu, Karan Goel, and Christopher Ré. Efficiently Modeling Long Sequences with Structured State Spaces. In *The Tenth International Conference on Learning Representations*, 2022a.

Albert Gu, Ankit Gupta, Karan Goel, and Christopher Re. On the Parameterization and Initialization of Diagonal State Space Models. In *Advances in Neural Information Processing Systems*, volume 35, pp. 35971–35983, 2022b.

Ankit Gupta, Albert Gu, and Jonathan Berant. Diagonal state spaces are as effective as structured state spaces. In *Advances in Neural Information Processing Systems*, volume 35, pp. 22982–22994, 2022.

David Ha and Jürgen Schmidhuber. Recurrent World Models Facilitate Policy Evolution. In *Advances in Neural Information Processing Systems*, volume 31, 2018.

Tuomas Haarnoja, Aurick Zhou, Pieter Abbeel, and Sergey Levine. Off-Policy Maximum Entropy Deep Reinforcement Learning with a Stochastic Actor. In *Proceedings of the 35th International Conference on Machine Learning*, pp. 1861–1870, 2018.

Danijar Hafner, Timothy Lillicrap, Ian Fischer, Ruben Villegas, David Ha, Honglak Lee, and James Davidson. Learning Latent Dynamics for Planning from Pixels. In *Proceedings of the 36th International Conference on Machine Learning*, volume 97, pp. 2555–2565. PMLR, 2019.

Danijar Hafner, Timothy Lillicrap, Jimmy Ba, and Mohammad Norouzi. Dream to Control: Learning Behaviors by Latent Imagination. In *8th International Conference on Learning Representations*, 2020.

Danijar Hafner, Timothy Lillicrap, Mohammad Norouzi, and Jimmy Ba. Mastering Atari with Discrete World Models. In *9th International Conference on Learning Representations*. arXiv, 2021. URL http://arxiv.org/abs/2010.02193. arXiv:2010.02193 [cs, stat].

Danijar Hafner, Jurgis Pasukonis, Jimmy Ba, and Timothy Lillicrap. Mastering Diverse Domains through World Models, April 2024. URL http://arxiv.org/abs/2301.04104. arXiv:2301.04104 [cs, stat].

Sili Huang, Jifeng Hu, Zhejian Yang, Liwei Yang, Tao Luo, Hechang Chen, Lichao Sun, and Bo Yang. Decision Mamba: Reinforcement Learning via Hybrid Selective Sequence Modeling, May 2024. URL http://arxiv.org/abs/2406.00079. arXiv:2406.00079 [cs].

Lukasz Kaiser, Mohammad Babaeizadeh, Piotr Milos, Blazej Osinski, Roy H. Campbell, Konrad Czechowski, Dumitru Erhan, Chelsea Finn, Piotr Kozakowski, Sergey Levine, Afroz Mohiuddin, Ryan Sepassi, George Tucker, and Henryk Michalewski. Model-Based Reinforcement Learning for Atari. In *International Conference on Learning Representations*, 2020.

Diederik P. Kingma and Max Welling. Auto-Encoding Variational Bayes, 2013. URL http://arxiv.org/abs/1312.6114. arXiv:1312.6114 [cs, stat].

Chris Lu, Yannick Schroecker, Albert Gu, Emilio Parisotto, Jakob Foerster, Satinder Singh, and Feryal Behbahani. Structured State Space Models for In-Context Reinforcement Learning. In *Thirty-seventh Conference on Neural Information Processing Systems*, 2023.

Marlos C. Machado, Marc G. Bellemare, Erik Talvitie, Joel Veness, Matthew Hausknecht, and Michael Bowling. Revisiting the Arcade Learning Environment: Evaluation Protocols and Open Problems for General Agents. *Journal of Artificial Intelligence Research*, 61:523–562, March 2018. ISSN 1076-9757. doi: 10.1613/jair.5699. URL https://jair.org/index.php/jair/article/view/11182.

Vincent Micheli, Eloi Alonso, and François Fleuret. Transformers are Sample-Efficient World Models. In *International Conference on Learning Representations*, March 2023.

Volodymyr Mnih, Koray Kavukcuoglu, David Silver, Alex Graves, Ioannis Antonoglou, Daan Wierstra, and Martin Riedmiller. Playing Atari with Deep Reinforcement Learning, December 2013. URL http://arxiv.org/abs/1312.5602. arXiv:1312.5602 [cs].

Aaron van den Oord, Oriol Vinyals, and Koray Kavukcuoglu. Neural Discrete Representation Learning, May 2018. URL http://arxiv.org/abs/1711.00937. arXiv:1711.00937 [cs].

Toshihiro Ota. Decision Mamba: Reinforcement Learning via Sequence Modeling with Selective State Spaces, March 2024. URL http://arxiv.org/abs/2403.19925. arXiv:2403.19925 [cs].

Jan Robine, Marc Höftmann, Tobias Uelwer, and Stefan Harmeling. Transformer-based World Models Are Happy With 100k Interactions. In *International Conference on Learning Representations*, March 2023.

Mohammad Reza Samsami, Artem Zholus, Janarthanan Rajendran, and Sarath Chandar. Mastering Memory Tasks with World Models. In *The International Conference on Learning Representations*, March 2024.

Julian Schrittwieser, Ioannis Antonoglou, Thomas Hubert, Karen Simonyan, Laurent Sifre, Simon Schmitt, Arthur Guez, Edward Lockhart, Demis Hassabis, Thore Graepel, Timothy Lillicrap, and David Silver. Mastering Atari, Go, chess and shogi by planning with a learned model. *Nature*, 588(7839):604–609, December 2020. ISSN 0028-0836, 1476-4687. doi: 10.1038/s41586-020-03051-4. URL https://www.nature.com/articles/s41586-020-03051-4.

John Schulman, Filip Wolski, Prafulla Dhariwal, Alec Radford, and Oleg Klimov. Proximal Policy Optimization Algorithms, August 2017. URL http://arxiv.org/abs/1707.06347. arXiv:1707.06347 [cs].

Max Schwarzer, Ankesh Anand, Rishab Goel, R. Devon Hjelm, Aaron Courville, and Philip Bachman. Data-Efficient Reinforcement Learning with Self-Predictive Representations. In *9th International Conference on Learning Representations*, 2021.

David Silver, Aja Huang, Chris J. Maddison, Arthur Guez, Laurent Sifre, George Van Den Driessche, Julian Schrittwieser, Ioannis Antonoglou, Veda Panneershelvam, Marc Lanctot, Sander Dieleman, Dominik Grewe, John Nham, Nal Kalchbrenner, Ilya Sutskever, Timothy Lillicrap, Madeleine Leach, Koray Kavukcuoglu, Thore Graepel, and Demis Hassabis. Mastering the game of Go with deep neural networks and tree search. *Nature*, 529(7587):484–489, 2016. ISSN 0028-0836, 1476-4687. doi: 10.1038/nature16961. URL https://www.nature.com/articles/nature16961.

David Silver, Julian Schrittwieser, Karen Simonyan, Ioannis Antonoglou, Aja Huang, Arthur Guez, Thomas Hubert, Lucas Baker, Matthew Lai, Adrian Bolton, Yutian Chen, Timothy Lillicrap, Fan Hui, Laurent Sifre, George Van Den Driessche, Thore Graepel, and Demis Hassabis. Mastering the game of Go without human knowledge. *Nature*, 550(7676):354–359, October 2017. ISSN 0028-0836, 1476-4687. doi: 10.1038/nature24270. URL https://www.nature.com/articles/nature24270.

Jimmy TH Smith, Andrew Warrington, and Scott W Linderman. Simplified state space layers for sequence modeling. In *The Eleventh International Conference on Learning Representations*, 2023.

Richard S. Sutton and Andrew G. Barto. *Reinforcement learning: an introduction*. Adaptive computation and machine learning. MIT Press, Cambridge, Mass, 1998. ISBN 978-0-262-19398-6.

Alexandre Torres–Leguet. mamba.py: A simple, hackable and efficient Mamba implementation in pure PyTorch and MLX., 2024. URL https://github.com/alxndrTL/mamba.py.

Raf Vandebril, M Van Barel, Gene Golub, and Nicola Mastronardi. A bibliography on semiseparable matrices. *Calcolo*, 42:249–270, 2005. Publisher: Springer.

Ashish Vaswani, Noam Shazeer, Niki Parmar, Jakob Uszkoreit, Llion Jones, Aidan N Gomez, Łukasz Kaiser, and Illia Polosukhin. Attention is All you Need. In *Advances in Neural Information Processing Systems*, volume 30, 2017.

Weipu Zhang, Gang Wang, Jian Sun, Yetian Yuan, and Gao Huang. STORM: Efficient Stochastic Transformer based World Models for Reinforcement Learning. In *Thirty-seventh Conference on Neural Information Processing Systems*, 2023.

Lianghui Zhu, Bencheng Liao, Qian Zhang, Xinlong Wang, Wenyu Liu, and Xinggang Wang. Vision Mamba: Efficient Visual Representation Learning with Bidirectional State Space Model. In *Proceedings of the 41st International Conference on Machine Learning*, volume 235 of *Proceedings of Machine Learning Research*, pp. 62429–62442. PMLR, July 2024. URL https://proceedings.mlr.press/v235/zhu24f.html.

A APPENDIX

A.1 ATARI100K LEARNING CURVES

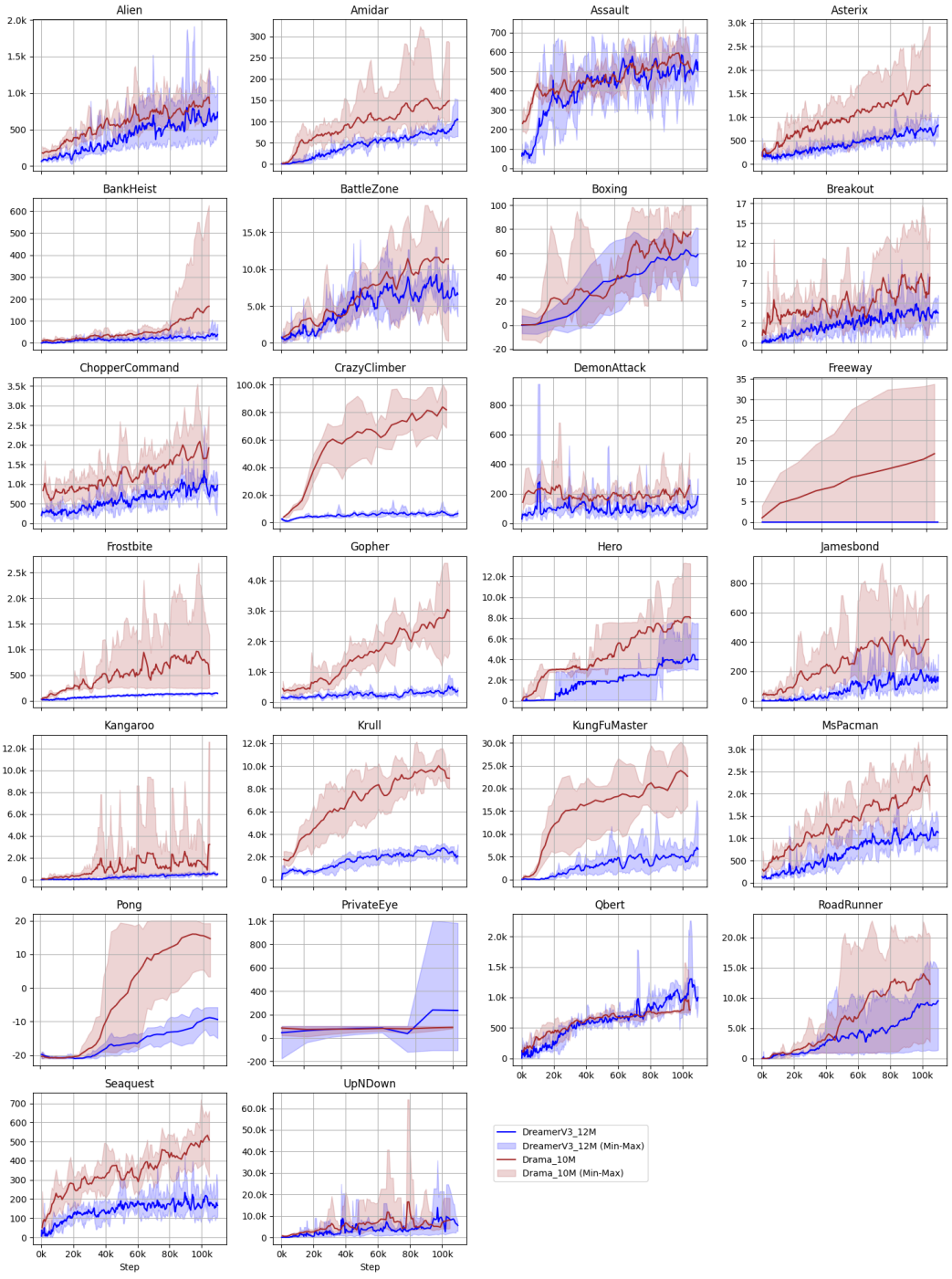

Figure 4: Atari100k Learning Curve. Drama vs. DreamerV3 with few parameters. The size of DreamerV3 is 12 millions and the size of Drama is 10 millions.

Game	Random	Human	DramaXS	DreamerV3XS
Alien	228	7128	**820**	553
Amidar	6	1720	**131**	79
Assault	222	742	**539**	489
Asterix	210	8503	**1632**	669
BankHeist	14	753	**137**	27
BattleZone	2360	37188	**10860**	5347
Boxing	0	12	**78**	60
Breakout	2	30	**7**	4
ChopperCommand	811	7388	**1642**	1032
CrazyClimber	10780	35829	**52242**	7466
DemonAttack	152	1971	**201**	64
Freeway	0	30	**15**	0
Frostbite	65	4335	**785**	144
Gopher	258	2412	**2757**	287
Hero	1027	30826	**7946**	3972
Jamesbond	29	303	**372**	142
Kangaroo	52	3035	**1384**	584
Krull	1598	2666	**9693**	2720
KungFuMaster	258	22736	**17236**	4282
MsPacman	307	6952	**2270**	1063
Pong	-21	15	**15**	-10
PrivateEye	25	69571	90	**207**
Qbert	164	13455	796	**983**
RoadRunner	12	7845	**14020**	8556
Seaquest	68	42055	**497**	169
UpNDown	533	11693	**7387**	6511
Normalised Mean (%)	0	100	105	37
Normalised Median (%)	0	100	27	7

Table 3: Atari100K performance table. Drama achieves significantly better performance than DreamerV3 in small model domains within model-based reinforcement learning, highlighting the parameter efficiency of Mamba-powered MBRL.

A.2 UNIFORM SAMPLING VS. DFS LEARNING CURVES

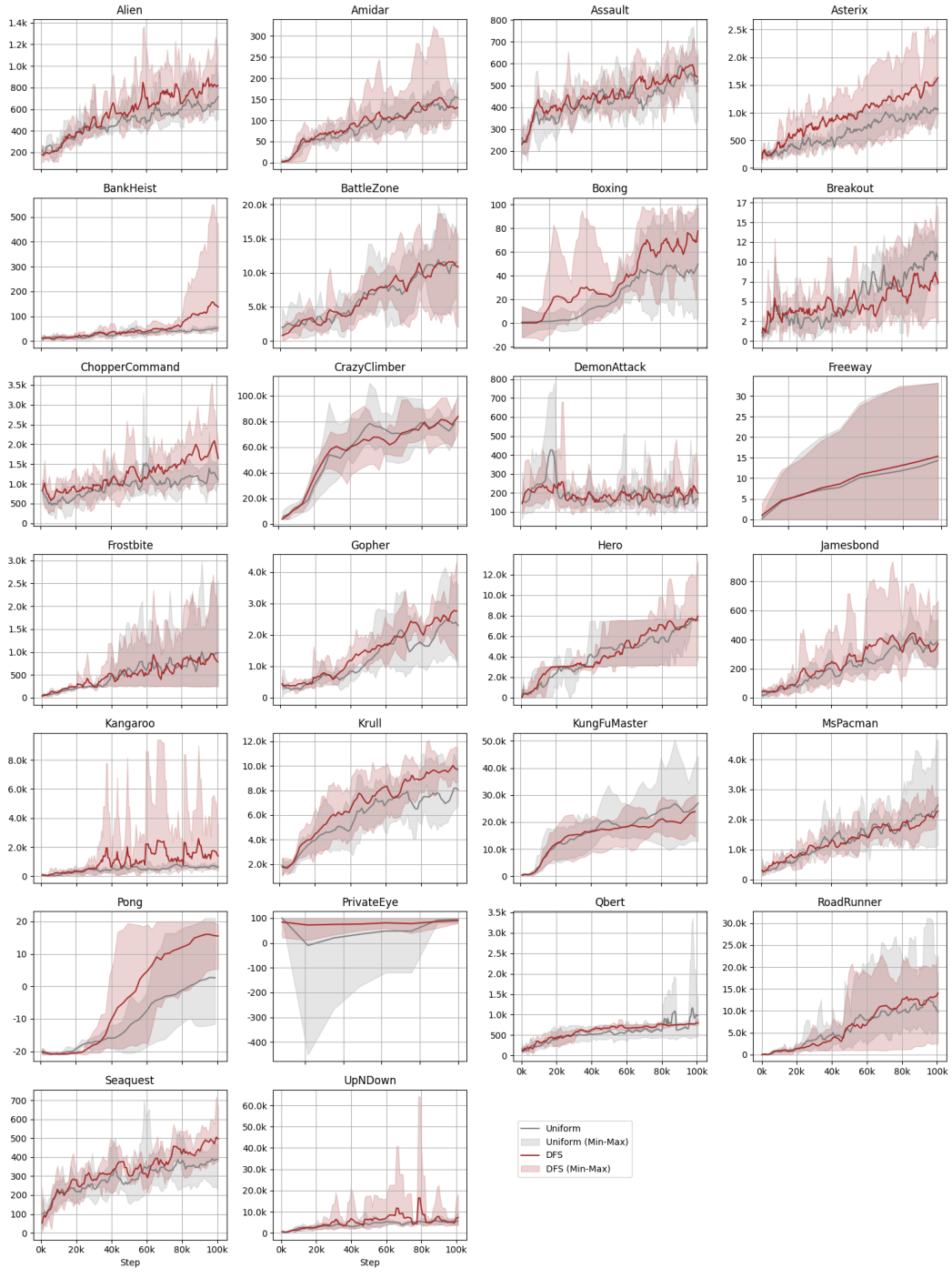

Figure 5: Uniform Sampling vs. DFS Learning Curve.

Game	Random	Human	DFS	Uniform
Alien	228	7128	**820**	696
Amidar	6	1720	131	**154**
Assault	222	742	**539**	511
Asterix	210	8503	**1632**	1045
BankHeist	14	753	**137**	52
BattleZone	2360	37188	10860	**10900**
Boxing	0	12	**78**	49
Breakout	2	30	7	**11**
ChopperCommand	811	7388	**1642**	1083
CrazyClimber	10780	35829	52242	**77140**
DemonAttack	152	1971	**201**	151
Freeway	0	30	**15**	15
Frostbite	65	4335	785	**975**
Gopher	258	2412	**2757**	2289
Hero	1027	30826	**7946**	7564
Jamesbond	29	303	**372**	363
Kangaroo	52	3035	**1384**	620
Krull	1598	2666	**9693**	7553
KungFuMaster	258	22736	17236	**24030**
MsPacman	307	6952	2270	**2508**
Pong	-21	15	**15**	3
PrivateEye	25	69571	**90**	76
Qbert	164	13455	796	**939**
RoadRunner	12	7845	**14020**	9328
Seaquest	68	42055	**497**	384
UpNDown	533	11693	**7387**	5756
Normalised Mean (%)	0	100	105	80
Normalised Median (%)	0	100	27	28

Table 4: The Atari100K performance table demonstrates that the Drama XS model, when paired with DFS, achieves a higher normalized mean score compared to using the uniform sampling method. This highlights the effectiveness of DFS in enhancing performance on Atari100K benchmarks within Mamba-powered MBRL.

A.3 More trainable parameters

As model-based RL agents consist of multiple trainable components, tuning the hyperparameters for each part can be resource-intensive and is not the primary focus of this research. Previous work has demonstrated that increasing the neural network's size often leads to stronger performance on benchmarks Hafner et al. (2024). In Figure 6, we demonstrate that Drama achieves overall better performance when using a more robust auto-encoder and a larger SSM hidden state dimension n. Notably, the S model exhibits significantly improved results in games like `Breakout` and `BankHeist`, where pixel-level information plays a crucial role.

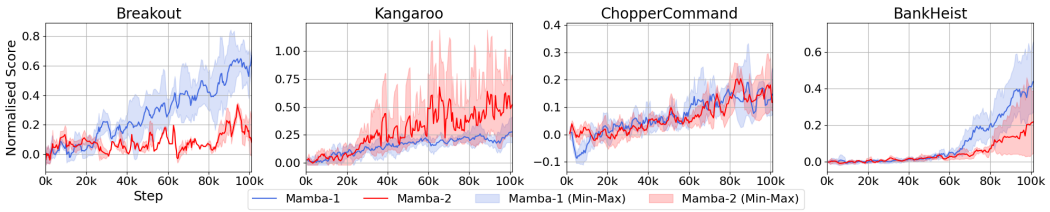

Figure 6: S model vs. XS model. We adjusted the game set to emphasise the importance of recognising small objects. The S model features a more robust auto-encoder than the XS model, with additional filters and 3M more trainable parameters. In terms of performance, the S model significantly outperforms the XS model in `Breakout` and `BankHeist`. However, it underperforms in `Kangaroo` and shows comparable performance in `ChopperCommand`.

A.4 Loss and Hyperparameters

A.4.1 Variational Auto-encoder

The hyperparameters shown in Table 5 correspond to the default model, also referred to as XS in Figure 6. For the S model, we simply double the number of filters per layer to obtain a stronger auto-encoder.

Hyperparameter	Value
Frame shape (h, w, c)	(64, 64, 3)
Layers	5
Filters per layer (Encoder)	(16, 32, 48, 64, 64)
Filters per layer (Decoder)	(64, 64, 48, 32, 16)
Kernel	5
Act	SiLU
Batch Norm	Yes

Table 5: Hyperparameters for the auto-encoder.

A.4.2 Mamba-1 and Mamba-2

Similar to the previous section, the values shown in Table 6 correspond to the default model. For the S model, we double the latent state dimension, allowing more relevant information to be stored in the recurrent state. In the Mamba-2 model, the enhanced architecture supports a larger latent state dimension without significantly increasing the training time.

Hyperparameter	Value
Hidden state dimension (d)	512
Layers	2
Latent state dimension (n)	16
RMS Norm	True
Act	SiLU
Mamba-2: Head dimension (p)	128

Table 6: Hyperparameters for Mamba-1 and Mamba-2. Except the head dimension is only for Mamba-2, the other hyperparameters are shared. The head number is 512/128 = 4.

A.4.3 REWARD AND TERMINATION PREDICTION HEADS

Both the reward and termination flag predictors take the deterministic state output from the dynamic model to make their predictions. Due to the quality of the hidden state extracted by the dynamic model, a single fully connected layer is sufficient for accurate predictions.

Hyperparameter	Value
Hidden units	256
Layers	1

Table 7: Hyperparameters for reward and termination prediction heads.

The world model is optimized in an end-to-end and self-supervised manner on batches of shape (b, l) drawn from the experience replay.

$$\mathcal{L}(\omega) = \mathbb{E}\left[\sum_{i=1}^{l} \underbrace{(O_i - \hat{O}_i)^2}_{\text{reconstruction loss}} + \mathcal{L}_{dyn}(\omega) + 0.1 * \mathcal{L}_{rep}(\omega) - \underbrace{\ln p(\hat{r}_i | d_i; \omega)}_{\text{reward prediction loss}} - \underbrace{\ln p(\hat{t}_i | d_i; \omega)}_{\text{termination prediction loss}}\right] \tag{6}$$

where

$$\begin{aligned} \mathcal{L}_{\text{dyn}}(\omega) &= \max\left(1, \text{KL}\left[\text{sg}(p(\boldsymbol{z}_{i+1} | \mathbf{O}_{i+1}; \omega)) \parallel q(\hat{\boldsymbol{z}}_{i+1} | d_i; \omega)\right]\right) \\ \mathcal{L}_{rep}(\omega) &= \max\left(1, \text{KL}\left[p(\boldsymbol{z}_{i+1} | \mathbf{O}_{i+1}; \omega) \parallel \text{sg}(q(\hat{\boldsymbol{z}}_{i+1} | d_i; \omega))\right]\right) \end{aligned} \tag{7}$$

and $\text{sg}(\cdot)$ represents the stop gradient operation.

A.4.4 ACTOR CRITIC HYPERPARAMETERS

We adopt the behavior policy learning setup from DreamerV3 (Hafner et al., 2024) for simplicity and strong performance, as the behaviour policy model is not central to our main contribution.

Hyperparameter	Value
Layers	2
Gamma	0.985
Lambda	0.95
Entropy coefficient	3e-4
Max gradient norm	100
Actor hidden units	256
Critic hidden units	512
RMS Norm	True
Act	SiLU
Batch size (b_{img})	1024
Imagine context length (l_{img})	8

Table 8: Hyperparameters for the behaviour policy.

A.5 PSEUDOCODE OF DRAMA

Algorithm 1 Training the world model and the behaviour policy

Require: Initialize behavior policy π_θ, world model f_ω, and replay buffer $\mathcal{E}$

Loop:
  Phase 1: Data Collection
    Collect experience tuple $(\mathbf{O}_t, a_t, r_t, e_t)$ using π_θ
    Store $(\mathbf{O}_t, a_t, r_t, e_t)$ into replay buffer $\mathcal{E}$
  Phase 2: World Model Training
    Sample b trajectories of length l from $\mathcal{E}$
    Update world model f_ω using sampled trajectories
  Phase 3: Behaviour Model Training
    Sample b_{img} trajectories of length l_{img} from $\mathcal{E}$
    Retrieve context from the first $l_{\text{img}} - 1$ experiences from the world model f_ω
    Generate imagined rollout for h steps using the last experience
    Train behavior policy π_θ with imagined rollout
Repeat

A.6 THE GRID WORLD ERROR CALCULATION

The Grid World environment task requires the dynamics model to capture two types of sequences. The first, referred to as the *geometric sequence*, involves reconstructing the structural features of the map. The map is surrounded by black walls, with only one agent and one goal cell in the center, while the remaining cells are plain floor tiles. Formally, let the map M be defined as a grid where $M[i, j]$ represents the cell at position (i, j). The geometric sequence requires the dynamics model to encode the spatial relationships such that $M[i, j]$ satisfies the constraints of walls (W), floor (F), agent (A), and goal (G), with walls forming the boundary:

$$M[i,j] = \begin{cases} W, & \text{if } (i = 0 \text{ or } i = l_g - 1) \text{ or } (j = 0 \text{ or } j = l_g - 1), \\ F, & \text{if } (i,j) \notin \{W, A, G\}, \\ A, & \text{if } (i,j) = \text{agent position}, \\ G, & \text{if } (i,j) = \text{goal position}. \end{cases}$$

Therefore, the geometric error E_g is defined as instances where $M[i, j] \neq W$ for boundary cells, i.e., when $(i = 0 \text{ or } i = l_g - 1)$ or $(j = 0 \text{ or } j = l_g - 1)$. For interior cells, where $0 < i < l_g - 1$ and $0 < j < l_g - 1$, there must be exactly one agent and one goal, with all remaining cells being floors.

The second component, referred to as the *logic sequence*, involves predicting the correct next position of the agent A_t based on the prior action a_{t-1} in the sequence. This prediction requires the model to retain information about the previous action, reconstruct the geometric sequence, and determine the agent's subsequent position accordingly. The logic error, E_l, is defined as an incorrect prediction of the next position. Specifically, the auto-generated action must meet two criteria: (1) it must be valid, ensuring only one agent occupies the interior cells, and (2) the predicted next position of the agent must match the position in the subsequent frame. If either condition is violated, the prediction is marked as incorrect.

The **Error (%)** presented in Table 2 represents the average of E_g and E_l.

A.7 EXPERIMENT 'IMAGINATION' FIGURES

In this section, we analyze reconstructed frames generated by the 'imagination' of the dynamics model to investigate potential causes of its poor performance in certain games, such as `Breakout`.

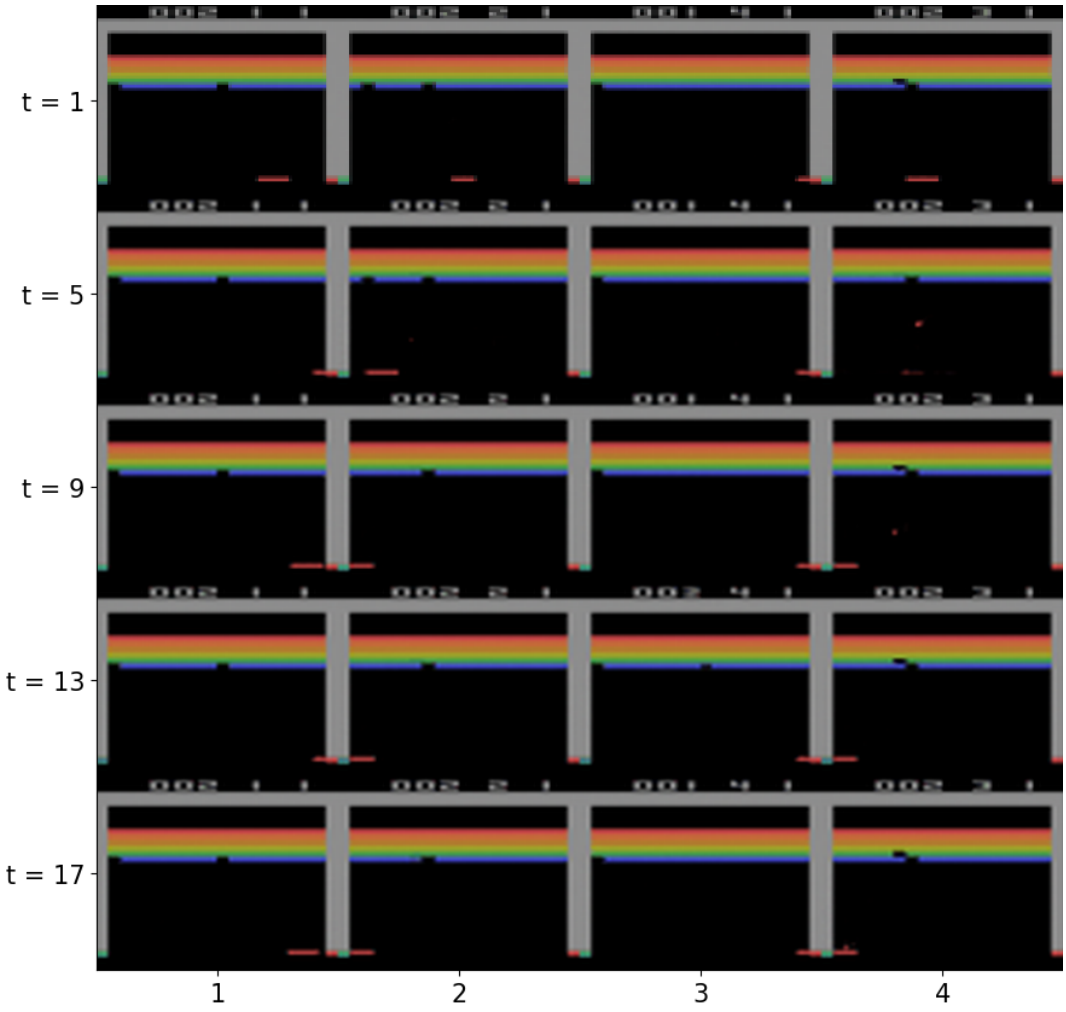

Figure 7: Drama XS model's 'imagination' in `Breakout`. The model performs poorly in `Breakout`, as the reconstructed frames from the autoregressive generation frequently fail to include the ball, a critical game element. This omission likely contributes to its subpar performance.

The differences in reconstructed frames, as shown in Figure 7 and Figure 8, along with the performance improvements depicted in Figure 6, suggest that employing a more robust autoencoder may aid in better handling tasks that pixel-level information is crucial. Supporting this observation, the Drama XS model performs relatively well in `Pong`, as shown in Figure 9, a game that shares similar features with `Breakout` (paddles and balls) but is less visually complex due to the absence of colourful bricks. While further investigation is warranted, this indicates that improving the autoencoder could be a promising initial step in addressing performance limitations in such tasks.

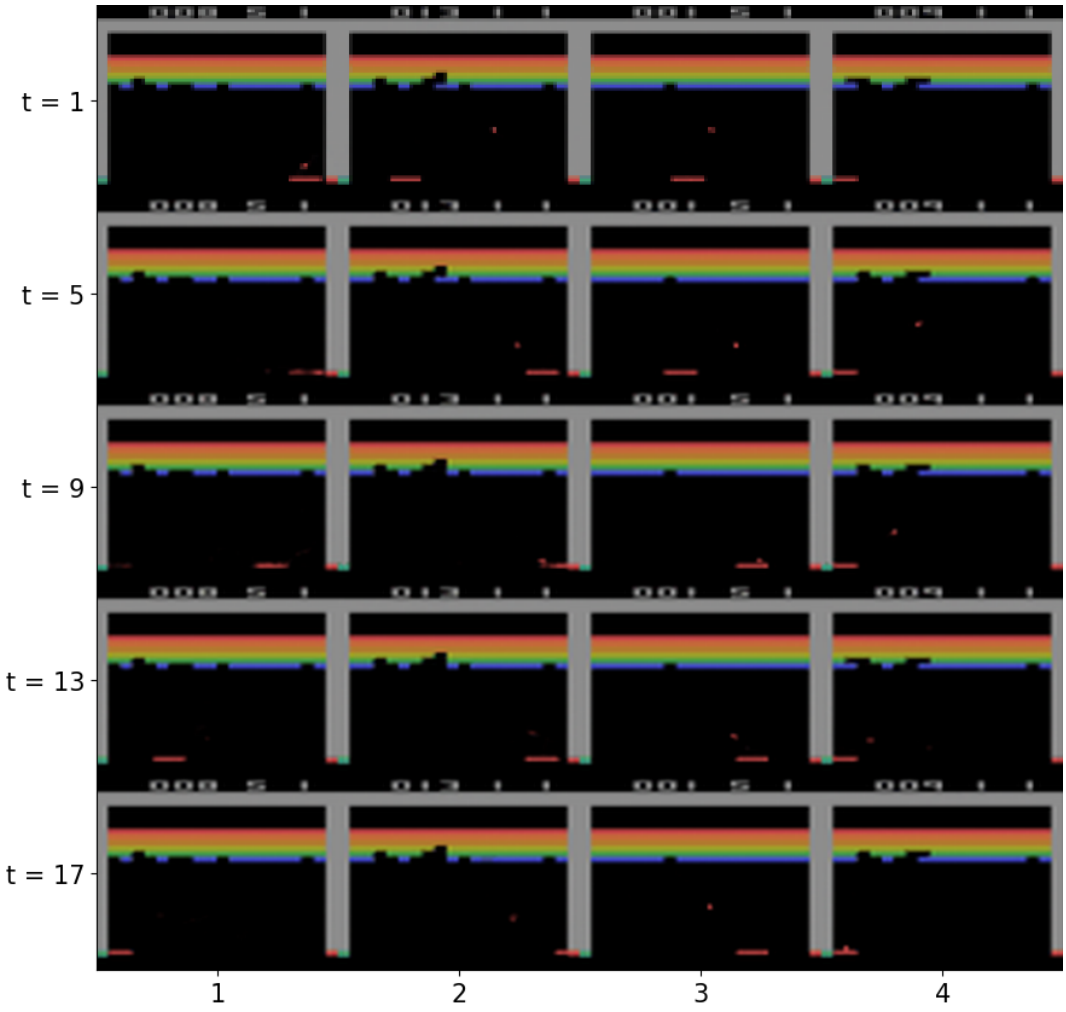

Figure 8: Drama S model's 'imagination' in `Breakout` demonstrates significant improvements compared to the XS model. The ball is successfully included in most of the reconstructed frames.

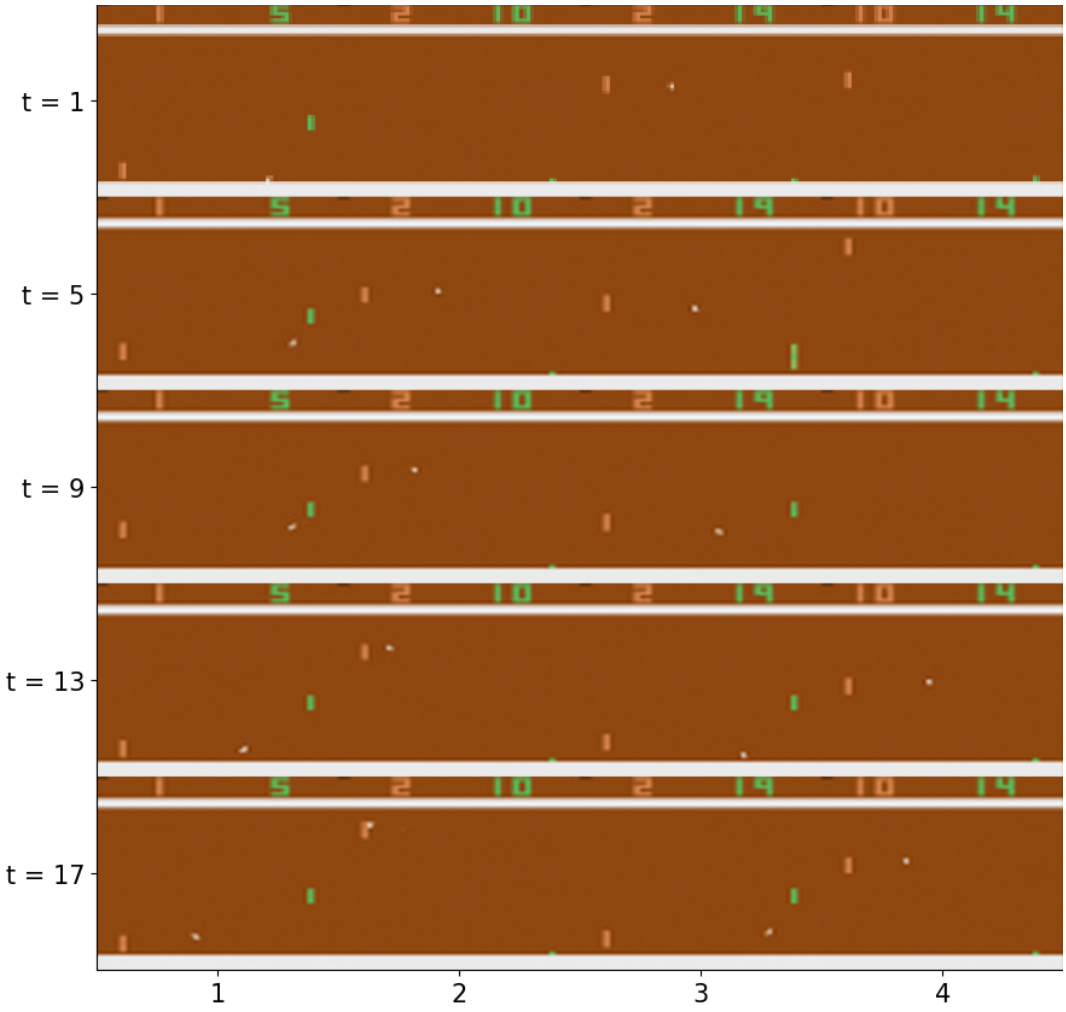

Figure 9: Drama XS model's 'imagination' in `Pong` demonstrates a notable contrast to its performance in `Breakout`, as the model performs well in `Pong`. Although the two games share some similarities, `Pong` lacks the colourful bricks present in `Breakout`, resulting in reduced visual complexity. Consequently, the model faces less pressure in encoding frames, and the ball is included in most of the 'imagined' frames.

A.8 Wall-Clock Time Comparison of Dynamic Models in MBRL

As shown in Figure 10, we compare the wall-clock time of different dynamics models in the Atari100k MBRL task. The figure highlights that both Mamba-1 and Mamba-2 are more efficient than the Transformer during the 'imagination' phase for the tested sequence lengths. Regarding training time, Mamba-2 shows a slight disadvantage with shorter training sequences but surpasses both the Transformer and Mamba-1 when training sequences are longer. This makes Mamba-2 particularly advantageous for tasks requiring effective modelling of long sequences. All dynamics models were tested under identical conditions with comparable training parameter sizes.

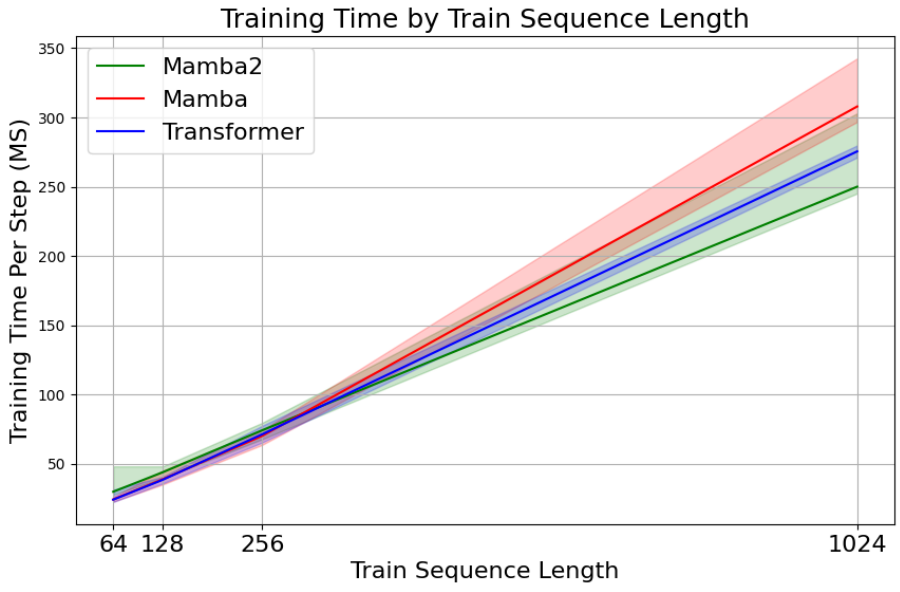

(a)

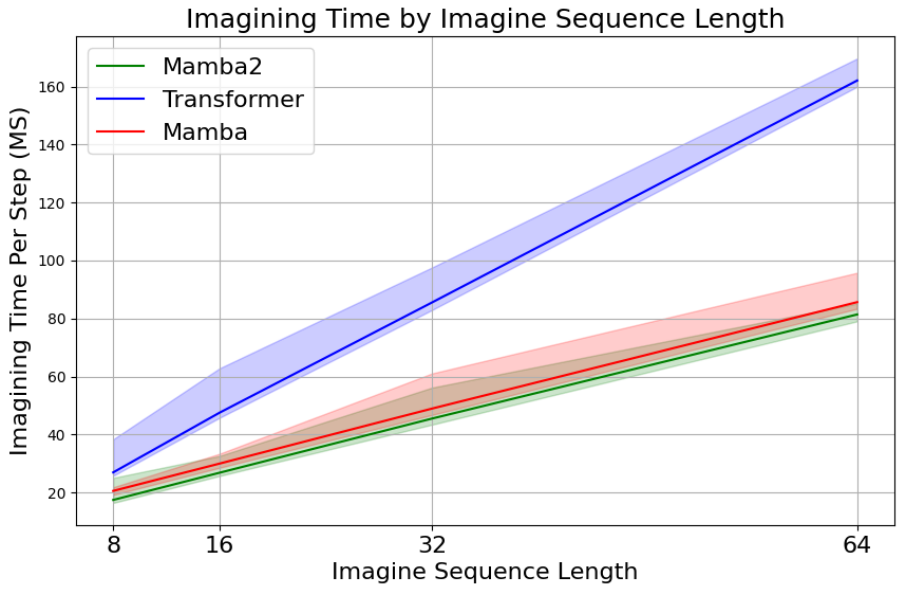

(b)

Figure 10: Wall-clock time for training and imagining with different dynamics models in MBRL was measured. The experiments were conducted on a laptop equipped with an NVIDIA RTX 2000 Ada Mobile GPU. Notably, the Transformer model in this experiment utilised a KV Cache to accelerate inference.